A role of reactive oxygen species in apoptotic activation of volume-sensitive Cl^- channel

Takahiro Shimizu, Tomohiro Numata, and Yasunobu Okada*

Department of Cell Physiology, National Institute for Physiological Sciences, and Japan Science and Technology Agency, Okazaki 444-8585, Japan

Communicated by Setsuro Ebashi, National Institute for Physiological Sciences, Okazaki, Japan, March 11, 2004 (received for review March 8, 2004)

Apoptotic volume decrease is a pivotal event triggering a cell to undergo apoptosis and is induced by ionic effluxes resulting mainly from increased K^+ and Cl^- conductances. Here, we demonstrate that in human epithelia HeLa cells both mitochondrion- and death receptor-mediated apoptosis inducers [staurosporine and Fas ligand or tumor necrosis factor (TNF)-α] rapidly activate Cl^- currents that show properties phenotypical of volume-sensitive outwardly rectifying Cl^- channel currents, including outward rectification, voltage-dependent inactivation gating at large positive potentials, inhibition by osmotic shrinkage, sensitivity to classic Cl^- channel blockers, and dependence on cytosolic ATP. Staurosporine, but not Fas ligand or TNF-α, rapidly (within 30 min) increased the intracellular level of reactive oxygen species (ROS). A ROS scavenger and an NAD(P)H oxidase inhibitor blocked the current activation by staurosporine but not by Fas ligand or TNF-α. A ROS scavenger also inhibited apoptotic volume decrease, caspase-3 activation, and apoptotic cell death induced by staurosporine. Thus, it is concluded that an apoptosis-triggering anion conductance is carried by the volume-sensitive outwardly rectifying Cl^- channel and that the channel activation on apoptotic stimulation with staurosporine, but not with Fas ligand or TNF-α, is mediated by ROS.

Apoptosis is a physiological/pathophysiological form of cell death, which is defined by biochemical and morphological changes including cell volume decrease, caspase activation, chromatin condensation, DNA laddering, and cell fragmentation. The apoptotic volume decrease (AVD) is an early-phase, essential component of the cascade leading to apoptotic cell death and is driven by osmolyte efflux resulting mainly from activation of K^+ and Cl^- conductances (1, 2). Actually, several studies have reported that Cl^- currents are activated on apoptotic stimulation (3–6), although little is known concerning the type of Cl^- channel and its activating signal. The involvement of the volume-sensitive outwardly rectifying (VSOR) Cl^- channel has been suggested on the basis of observations that induction of AVD is coupled to a facilitation of the regulatory volume decrease (RVD) and prevented by known blockers of VSOR but not of cAMP- and Ca^{2+}-activated Cl^- channels (7). Thus, the present study addresses questions as to whether the apoptosis-triggering anion channel exhibits volume sensitivity and properties phenotypical of the VSOR Cl^- channel, and what the upstream signal is for activation of this Cl^- channel under nonswelling conditions.

Materials and Methods

Cell Culture. Human cervix HeLa cells were grown as a monolayer in minimum essential medium (MEM) supplemented with 10% FBS, 40 IU/ml penicillin G, and 100 μg/ml streptomycin under a 95% air/5% CO_2 atmosphere. For electrophysiological experiments and cell volume measurements, cells were detached from the plastic substrate and cultured in suspension with agitation for 15–300 min in a CO_2 incubator. To induce apoptosis, HeLa cells were treated with 4 μM staurosporine (STS), 500 ng/ml anti-Fas antibody, or 2 ng/ml tumor necrosis factor (TNF)-α plus 1 μg/ml cycloheximide (TNF-α+CHX).

Patch-Clamp Experiments. Whole-cell recordings were performed at room temperature (22–26°C), as described (8), with spherical cells after detaching them from the chamber bottom by lifting with a patch pipette. When the extracellular Cl^- concentration was changed, a salt bridge containing 3 M KCl was used. To selectively record whole-cell Cl^- currents, NMDG-Cl-based solutions were used for pipette and bath solutions. The pipette (intracellular) solution contained 120 mM NMDG, 120 mM HCl, 1.5 mM $MgCl_2$, 1.5 mM Na_2ATP, 0.3 mM GTP, 1 mM EGTA, 5 mM Hepes, and 50 mM mannitol (pH 7.3, 300 mosmol/kg H_2O). The dependence of Cl^- channel activation on intracellular ATP was tested by omitting the compound from the pipette solution. The isotonic bathing solution contained 120 mM NMDG, 120 mM HCl, 0.5 mM $MgCl_2$, 1 mM $CaCl_2$, 5 mM Hepes, and 60 mM mannitol (pH 7.5, 305 mosmol/kg H_2O). For selectivity experiments, HCl was replaced with HI, HBr, or aspartic acid. When *N*-acetyl-cysteine (NAC) (10 mM) was added, the osmolality was adjusted by reducing the mannitol concentration. To prepare hypotonic (280 mosmol/kg H_2O) or hypertonic solution (355 mosmol/kg H_2O), the mannitol concentration of the control bathing solution was reduced or increased, respectively. The osmolality was measured by using a freezing-point depression osmometer (OM802, Vogel, Giessen, Germany).

Measurements of Intracellular Reactive Oxygen Species (ROS) Generation. The intracellular ROS level was detected by using 5-(and-6)-carboxy-2′,7′-dichlorodihydrofluorescein diacetate (carboxy-H_2DCFDA) (Molecular Probes) as reported (9). Carboxy-H_2DCFDA is a cell-permeable indicator for ROS that is nonfluorescent until the acetate groups are removed by intracellular esterases and oxidation occurs within the cell. When oxidized by various active oxygen species, it is irreversibly converted to the fluorescent form, DCF. For ROS measurements, cells were preincubated for 30 min with MEM containing 10 μM carboxy-H_2DCFDA. After detachment, cells were washed with isotonic solution that contained 95 mM NaCl, 4.5 mM KCl, 1 mM $MgCl_2$, 1 mM $CaCl_2$, 105 mM mannitol, and 5 mM Hepes (pH 7.3, 310 mosmol/kg H_2O) and plated into 96-well plates. Fluorescence was measured by a plate reader (Molecular Devices) with an excitation wavelength of 485 nm and an emission wavelength of 538 nm.

Cell Volume Measurements. Changes in cell volume were quantified by using an electronic sizing technique with a Coulter-type cell size analyzer (CDA-500, Sysmex, Kobe, Japan) as described (10). Isotonic or hypotonic solution consisted of 95 mM NaCl, 4.5 mM KCl, 1 mM $MgCl_2$, 1 mM $CaCl_2$, 10 mM $NaHCO_3$, 5 mM Hepes, and 105 or 0 mM mannitol, respectively (pH 7.3 adjusted

Abbreviations: AVD, apoptotic volume decrease; CHX, cycloheximide; DIDS, 4,4′-diisothiocyanatestilbene-2,2′-disulfonic acid; DPI, diphenylene-iodonium chloride; NAC, *N*-acetyl-cysteine; NPPB, 5-nitro-2-(3-phenylpropylamino) benzoic acid; ROS, reactive oxygen species; STS, staurosporine; TNF, tumor necrosis factor; VSOR, volume-sensitive outwardly rectifying.

*To whom correspondence should be addressed. E-mail: okada@nips.ac.jp.

www.pnas.org/cgi/doi/10.1073/pnas.0401604101

by NaOH; 310 or 200 mosmol/kg H_2O). During whole-cell recordings, cell size changes were also assessed by measuring the diameter of the spherical cell under a video microscope.

Caspase-3 Activity and Cell Viability Measurements. Caspase-3 activity was measured by using the CaspACE Assay System Fluorometric kit (Promega) as described (7). Cell viability was assessed by using the 3-(4,5-dimethylthiazol-2-yl)-2,5-diphenyl tetrazolium bromide (MTT) assay as described (7).

Statistics. Statistical differences of the data were evaluated by the paired or unpaired Student *t* test and were considered significant at $P < 0.05$.

Results and Discussion

Apoptosis Inducers Rapidly Activate VSOR Cl^- Channels. Most animal cells respond to a hypotonic challenge with the activation of K^+ and Cl^- conductances, which bring about the recovery of volume after osmotic swelling (11–13). Among the volume-regulatory Cl^- channels, the most ubiquitous type is the VSOR Cl^- channel (14), also called the volume-sensitive organic osmolyte and anion channel (VSOAC) (15) or the volume-regulated anion channel (VRAC) (16), which exhibits a number of phenotypical properties distinct from those of other types of anion channel (14–16). Human cervix epithelial HeLa cells also express this channel activity (17). Osmotic swelling induced by a hypotonic challenge (92% osmolality) brought about the activation of whole-cell Cl^- currents with properties phenotypical of VSOR Cl^- channel currents (14–16), including outward rectification, voltage-dependent inactivation gating at large positive potentials, inhibition by osmotic shrinkage, sensitivity to classic Cl^- channel blockers such as 5-nitro-2-(3-phenylpropylamino) benzoic acid (NPPB) and 4,4′-diisothiocyanatestilbene-2,2′-disulfonic acid (DIDS), and dependence on cytosolic ATP (Fig. 7, which is published as supporting information on the PNAS web site).

Stimulation of HeLa cells with a mitochondrion-mediated apoptosis inducer, STS, rapidly induced activation of whole-cell Cl^- currents (Fig. 1*A*) that was not accompanied by any significant changes in the mean cell diameter (97 ± 0.3% of the control, $n = 9$; $P > 0.05$). Even in the continued presence of STS, however, application of hypertonic solution (116% osmolality) that resulted in osmotic shrinkage (down to 91 ± 2% of the control, $n = 9$; $P < 0.05$) quickly suppressed Cl^- currents (Fig. 1*A*). The STS-induced Cl^- current exhibited voltage-dependent inactivation at large positive voltages (Fig. 1*B*) and outward rectification (Fig. 1*C*). This current was reversibly blocked by classic Cl^- channel antagonists (NPPB and DIDS) (Fig. 1*D*). Sensitivity to NPPB was independent of voltages, whereas that to DIDS was voltage-dependent with a more prominent inhibition at positive potentials. When cells were equilibrated with ATP-free pipette (intracellular) solution for over 15 min, STS failed to activate the Cl^- current (Fig. 1*D*). Normalized permeability coefficients for I^-, Br^-, Cl^-, and aspartate evaluated by their reversal potentials ($n = 6$) were 1.46 ± 0.03, 1.20 ± 0.01, 1, and 0.15 ± 0.01, respectively, corresponding to Eisenman's sequence I. These current properties are identical to those of VSOR Cl^- channel currents (refs. 14–16; also see Fig. 7) but distinct from those of currents from other known types of Cl^- channel (14, 18).

The death receptor-mediated apoptosis inducers, Fas ligand and TNF-α+CHX, also induced shrinkage-sensitive, NPPB-sensitive, and outwardly rectifying Cl^- currents (Fig. 2 *A* and *B*). Neither stimulation ever induced significant changes in the relative mean cell diameter (0.99 ± 0.01, $n = 10$ each; $P > 0.05$). These Cl^- currents always exhibited inactivation kinetics at large positive potentials (data not shown), voltage-dependent sensitivity to DIDS, and dependence on cytosolic ATP (Fig. 2 *C* and *D*), all of which are characteristics of VSOR Cl^- channel currents.

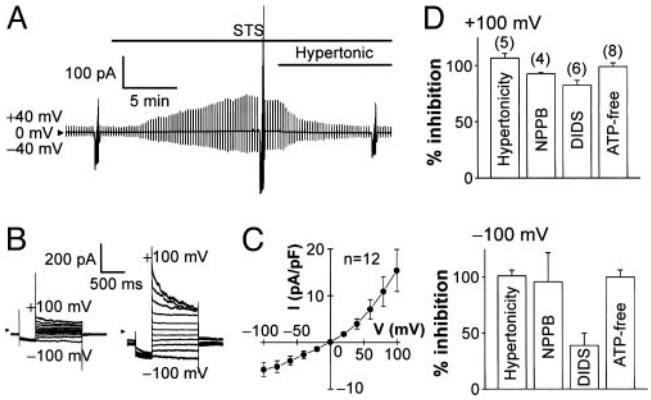

Fig. 1. Activation of VSOR Cl^- current by a mitochondrion-mediated apoptosis inducer, STS. (*A*) Representative record of whole-cell current before and during application of STS (4 μM), taken during application of alternating pulses from 0 to ±40 mV and, at selected time points, of step pulses from −100 to +100 mV in 20-mV increments. STS activated the current with a half activation time of 4.9 ± 0.5 min ($n = 12$). Note that the STS-induced current was inhibited by osmotic shrinkage induced by a hypertonic challenge. (*B*) Expanded traces of current responses to step pulses before (*Left*) and during (*Right*) stimulation with STS. Note that the STS-induced current exhibited faster inactivation kinetics at larger positive potentials. (*C*) I–V relationship for the mean densities of currents activated by STS. (*D*) Sensitivity of STS-induced current to shrinkage (induced by ≈5-min exposure to hypertonic solution of 116% osmolality), Cl^- channel blockers (≈5-min treatment with 100 μM NPPB and 500 μM DIDS), and cytosolic ATP removal (>15-min equilibration with ATP-free pipette solution). The percent of inhibition was calculated from the peak current densities recorded at ±100 mV from the cells under control (isotonic, ATP-containing, and blocker-free) conditions ($n = 27$) and the cells under hypertonic, cytosolic ATP-free, or blocker-containing conditions. Sensitivity to DIDS was voltage-dependent, being significantly lower at −100 mV than at +100 mV.

STS-Induced Activation of VSOR Cl^- Channel Is Mediated by ROS. STS is known to induce ROS generation (19–21), and so we examined the effects of a ROS scavenger, NAC, on STS-induced activation of VSOR Cl^- currents. As shown in Fig. 3*A*, STS-induced activation of VSOR Cl^- currents was almost completely (by 87.5 ± 18.6% at −100 mV and 101.1 ± 4.5% at +100 mV; $n = 5$) eliminated by this antioxidant. Sources of the oxygen free radicals may include the mitochondrial electron transport chain and a membrane-associated NAD(P)H oxidase system (22). A general inhibitor of NAD(P)H oxidases, diphenylene-iodonium chloride (DPI) (23), suppressed STS-induced activation of VSOR Cl^- current (Fig. 3*B*) by 70.6 ± 18.1 at −100 mV and 76.3 ± 14.6 at +100 mV ($n = 5$). In contrast, Fas ligand- or TNF-α-induced activation of VSOR Cl^- currents was not prevented by NAC (Figs. 3 *C* and *D*) or DPI (data not shown; $n = 3$). These results suggest that the effect of STS, but not that of Fas ligand or TNF-α, was mediated by ROS generated by NAD(P)H oxidases. Indeed, when using a membrane-permeable fluorescent probe, carboxy-H_2DCFDA, loaded into HeLa cells to monitor the level of ROS, we found that stimulation with STS quickly increased the intracellular level of ROS (Fig. 4*A*). STS-induced ROS production was inhibited by NAC and DPI (Fig. 4*A*) but not by an NO synthase inhibitor, N^{ω}-nitro-L-arginine methyl ester hydrochloride (L-NAME) (data not shown; $n = 24$).

Extracellular application of hydrogen peroxide (H_2O_2) increased the intracellular ROS level and augmented the STS-induced ROS increase in an additive manner (Fig. 4*B*). H_2O_2 was also found to directly activate Cl^- currents without producing

PHYSIOLOGY

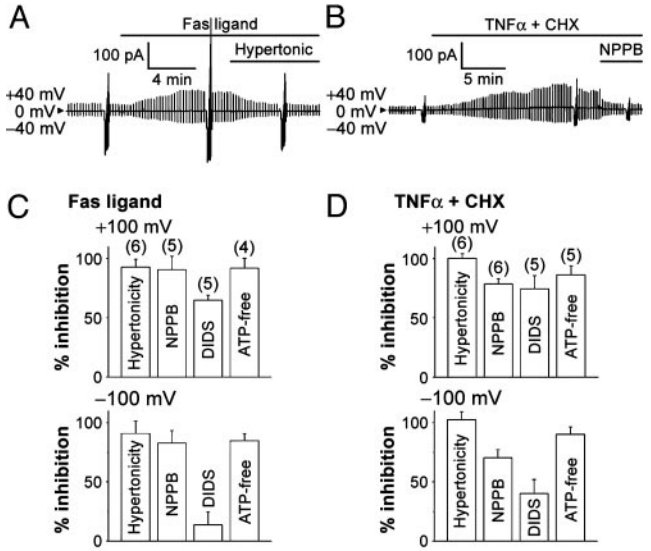

Fig. 2. Activation of VSOR Cl^- current by receptor-mediated apoptosis inducers. Clamped voltages are the same as in Fig. 1*A*. (*A*) Representative record of currents before and during application of anti-Fas antibody (500 ng/ml). Note the sensitivity of Fas ligand-induced current to osmotic shrinkage. (*B*) Representative record of currents before and during application of TNF-α (2 ng/ml) plus CHX (1 μg/ml). Note the sensitivity of TNF-α-induced current to NPPB (100 μM). (*C* and *D*) Sensitivity of currents activated by anti-Fas antibodies (*C*) and TNF-α+CHX (*D*) to osmotic shrinkage, NPPB, DIDS, and cytosolic ATP removal. The percent of inhibition was calculated by using the control data (n = 24 and 21 for *C* and *D*, respectively), as described in the legend for Fig. 1*D*. Significant voltage dependence was found only for sensitivity to DIDS.

any visible change in cell size (Fig. 5*A*). Like STS-induced Cl^- currents, H_2O_2-induced Cl^- currents could be inhibited by osmotic shrinkage (Fig. 5*A*) and exhibited voltage-dependent inactivation (Fig. 5*B*), outward rectification (Fig. 5*C*), voltage-independent sensitivity to both NPPB and cytosolic ATP removal, and voltage-dependent sensitivity to DIDS (Fig. 5*D*). These data indicate that ROS generation is an upstream signal in the STS-induced activation of the VSOR Cl^- channel.

Both receptor-mediated apoptosis inducers did significantly increase the level of ROS only after 5 h (Fig. 8, which is published as supporting information on the PNAS web site). This observation is in good agreement with previous reports (24–28). This ROS response to Fas ligand or TNF-α was NAC-sensitive (Fig. 8). However, neither Fas ligand nor TNF-α plus CHX signifi-

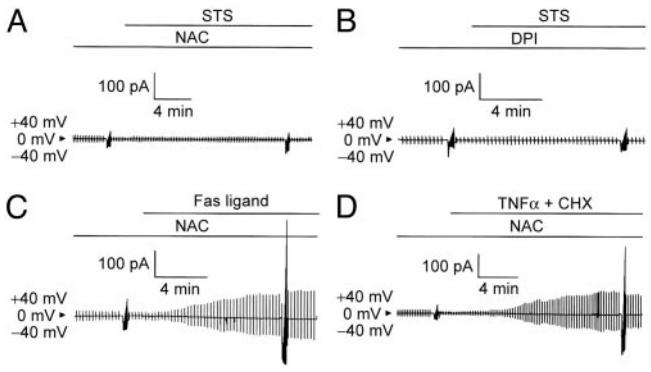

Fig. 3. Effects of a ROS scavenger (10 mM NAC in *A*, *C*, and *D*) and an NAD(P)H oxidase inhibitor (20 μM DPI in *B*) on STS-induced (*A* and *B*), Fas ligand-induced (*C*), or TNF-α-induced (*D*) activation of VSOR Cl^- current. Clamped voltages are the same as in Fig. 1*A*. Each trace represents five similar observations.

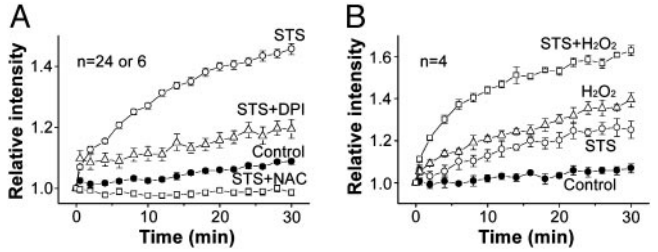

Fig. 4. ROS production by STS. (*A*) Effects of NAC (10 mM) and DPI (20 μM) on STS-induced ROS production monitored by DCF fluorescence. Each symbol represents the mean ± SEM (bar) of 24 observations except for experiments with DPI (n = 6). STS significantly increased the level of intracellular ROS ≥0.5 min after stimulation. NAC and DPI significantly inhibited this increase observed 0.5–30 and 4–30 min, respectively, after STS stimulation. DPI or NAC alone did not affect the ROS level in the absence of STS (data not shown, n = 6 or 24). (*B*) Effects of H_2O_2 (500 μM) on the ROS level in the absence and presence of STS. STS, H_2O_2, and STS plus H_2O_2 significantly increased the level observed 6–30, 2–30, and 2–30 min, respectively, after application.

cantly increased the ROS level within 30 min (data not shown; n = 16 or 12). This fact again precludes a possibility that ROS are involved in Fas ligand or TNF-α-induced activation of VSOR Cl^- channels.

STS-Induced Apoptotic Cell Death Is Mediated by ROS. Fig. 6*A* shows the time course of changes in the mean cell volume. AVD was rapidly induced by STS, as reported (7). The STS-induced AVD was abolished by DPI and NAC (Fig. 6*A*). Application of H_2O_2 also rapidly caused a significant decrease in the mean cell volume (Fig. 6*B*). More prominent AVD induction by STS compared to that by H_2O_2 may suggest an involvement of some ROS other than H_2O_2 (such as superoxide anions) in the STS-induced AVD induction mechanism. The STS-induced AVD was enhanced by coapplication of H_2O_2 (Fig. 6*B*). Application of STS induced activation of caspase-3 and marked reduction of cell viability after 4 and 8 h, respectively, as reported (7). NAC was found to markedly suppress STS-induced activation of caspase-3 (Fig. 6*C*)

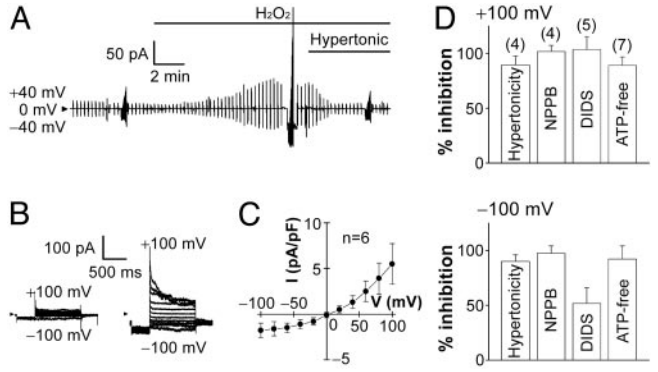

Fig. 5. Activation of VSOR Cl^- current by H_2O_2. (*A*) Representative record of whole-cell currents before and during application of H_2O_2 (500 μM). Clamped voltages are the same as in Fig. 1*A*. Note the sensitivity of H_2O_2-induced current to osmotic shrinkage. The relative mean cell diameter compared to the control (without H_2O_2) was 0.99 ± 0.01 (n = 7; $P > 0.05$) 3 min before and 0.92 ± 0.02 (n = 4; $P < 0.05$) 5 min after a hypertonic challenge in the presence of H_2O_2. (*B*) Expanded traces of current responses to step pulses before (*Left*) and during (*Right*) stimulation with H_2O_2. Note the voltage-dependent inactivation kinetics of H_2O_2-induced current. (*C*) I–V relationship for the mean densities of currents activated by H_2O_2. (*D*) Sensitivity of the H_2O_2-induced current to osmotic shrinkage, NPPB, DIDS, and cytosolic ATP removal. The percent of inhibition was calculated by using the control data (n = 19), as described in the legend for Fig. 1*D*. Note the voltage-dependent sensitivity to DIDS.

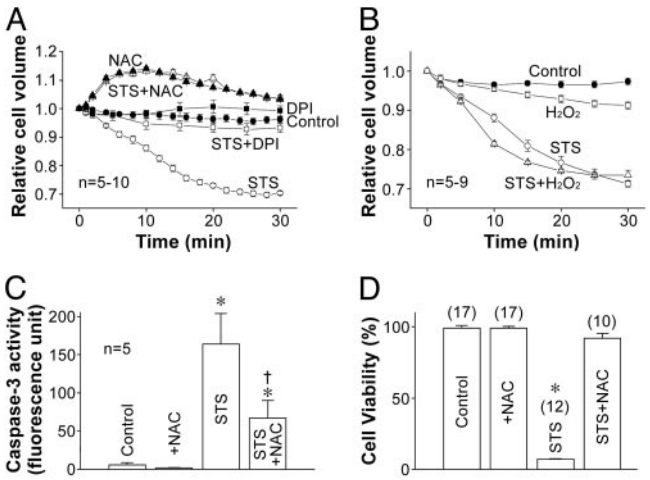

Fig. 6. Involvement of ROS in apoptotic events induced by STS. (*A*) Effects of NAC (10 mM) and DPI (20 μM) on induction of AVD by STS (4 μM). STS application caused significant decrease in the mean cell volume 1–30 min after stimulation with a half-maximum shrinkage time of 10.8 $\pm$ 0.7 min (n = 7). NAC and DPI significantly inhibited STS-induced AVD 2–30 and 5–30 min, respectively, after stimulation. NAC alone caused a significant increase in the mean cell volume, irrespective of STS stimulation. (*B*) Effects of H_2O_2 (500 μM) on mean cell volume and STS-induced AVD. H_2O_2 alone caused a significant decrease in the mean cell volume 10–30 min after stimulation. AVD induced by STS in the presence of H_2O_2 was of a significantly greater level than when H_2O_2 was absent, 5–15 min after stimulation. (*C*) Effects of NAC on activation of caspase-3 by 4-h application of STS. NAC significantly suppressed STS-induced caspase-3 activation. *, Significant difference between data with and without STS. †, Significant difference between data with and without NAC. (*D*) Effects of NAC on the induction of cell death by 8-h application of STS. Note the rescue from STS-induced cell death by NAC. *, Significantly different from the control cell viability.

and to prevent STS-induced cell death (Fig. 6*D*). A previous study of ours (29) showed that H_2O_2 increases the activity of caspase-3 in HeLa cells and decreases their viability. These observations indicate that some ROS-mediated event leads to caspase-3 activation and apoptotic cell death induced by STS.

Conclusion and Perspective. From the present study, the following two conclusions can be drawn. (*i*) Stimulation of either the mitochondrion-mediated or death receptor-mediated apoptotic pathway results in rapid activation of the VSOR Cl^- channel, which is involved in the induction of AVD in HeLa cells; and (*ii*) ROS serve as upstream signal in VSOR Cl^- channel activation by a mitochondrion-mediated apoptosis inducer, STS, but not by death receptor-mediated apoptosis inducers, Fas ligand and TNF-α. Further studies are required to determine what an upstream signal for activation of VSOR Cl^- channel by death receptor-mediated apoptosis inducers is. At present, it is also not known how ROS bring about activation of the VSOR Cl^- channel. There is a possibility that both ROS and death receptors stimulate an identical signal that is directly involved in activation of VSOR Cl^- channel. A Src-like tyrosine kinase, p56Lck, has been reported to mediate activation of an outwardly rectifying Cl^- channel in lymphocytes stimulated with Fas ligand (5). Caspase is known to be activated by ROS (29, 30) and to cleave p56Lck at the N-terminal domain (31, 32). However, it is well known that AVD occurs upstream of caspase activation (7, 33–35). Activation of AVD-inducing VSOR Cl^- channel is an early requisite event of apoptosis, because the block of this channel prevented cytochrome *c* release, caspase-3 activation, DNA laddering, and cell death (1, 7). Thus, identification of not only the VSOR Cl^- channel *per se* but also components of the molecular mechanism underlying its activation by apoptotic stimuli are of great importance, because these molecules may be promising targets for modulating apoptotic cell death in pathophysiological situations such as ischemia and tumorigenesis.

We thank R. Z. Sabirov for discussion and critical reading of the manuscript, E. L. Lee for reviewing the manuscript, M. Ohara and C. Kondo for technical assistance, and T. Okayasu for secretarial assistance. This work was supported by Grants-in-Aid for Scientific Research from the Ministry of Education, Culture, Sports, Science, and Technology of Japan and Japan Society for the Promotion of Science.

1. Okada, Y., Maeno, E., Shimizu, T., Dezaki, K., Wang, J. & Morishima, S. (2001) *J. Physiol. (London)* **532,** 3–16.
2. Gomez-Angelats, M. & Cidlowski, J. A. (2002) *Toxicol. Pathol.* **30,** 541–551.
3. Schumann, M. A., Gardner, P. & Raffin, T. A. (1993) *J. Biol. Chem.* **268,** 2134–2140.
4. Szabo, I., Lepple-Wienhues, A., Kaba, K. N., Zoratti, M., Gulbins, E. & Lang, F. (1998) *Proc. Natl. Acad. Sci. USA* **95,** 6169–6174.
5. Nietsch, H. H., Roe, M. W., Fiekers, J. F., Moore, A. L. & Lidofsky, S. D. (2000) *J. Biol. Chem.* **275,** 20556–20561.
6. Souktani, R., Berdeaux, A., Ghaleb, B., Giudicelli, J. F., Guize, L., Le Heuzey, J. Y. & Henry, P. (2000) *Am. J. Physiol.* **279,** C158–C165.
7. Maeno, E., Ishizaki, Y., Kanaseki, T., Hazama, A. & Okada, Y. (2000) *Proc. Natl. Acad. Sci. USA* **97,** 9487–9492.
8. Shimizu, T., Morishima, S. & Okada, Y. (2000) *J. Physiol. (London)* **528,** 457–472.
9. Wang, H. & Joseph, J. A. (1999) *Free Radical Biol. Med.* **27,** 612–616.
10. Hazama, A. & Okada, Y. (1988) *J. Physiol. (London)* **402,** 687–702.
11. Hoffmann, E. K. & Simonsen, L. O. (1989) *Physiol. Rev.* **69,** 315–382.
12. Okada, Y. & Hazama, A. (1989) *News Physiol. Sci.* **4,** 238–242.
13. Wehner, F., Olsen, H., Tinel, H., Kinne-Saffran, E. & Kinne, R. K. (2003) *Rev. Physiol. Biochem. Pharmacol.* **148,** 1–80.
14. Okada, Y. (1997) *Am. J. Physiol.* **273,** C755–C789.
15. Strange, K., Emma, F. & Jackson, P. S. (1996) *Am. J. Physiol.* **270,** C711–C730.
16. Nilius, B., Eggermont, J., Voets, T., Buyse, G., Manolopoulos, V. & Droogmans, G. (1997) *Prog. Biophys. Mol. Biol.* **68,** 69–119.
17. Diaz, M., Valverde, M. A., Higgins, C. F., Rucareanu, C. & Sepulveda, F. V. (1993) *Pflügers Arch.* **422,** 347–353.
18. Jentsch, T. J., Stein, V., Weinreich, F. & Zdebik, A. A. (2001) *Physiol. Rev.* **82,** 503–568.
19. Cai, J. & Jones, D. P. (1998) *J. Biol. Chem.* **273,** 11401–11404.
20. Kruman, I., Guo, Q. & Mattson, M. P. (1998) *J. Neurosci. Res.* **51,** 293–308.
21. Ahlemeyer, B. & Krieglstein, J. (1998) *Neurosci. Lett.* **246,** 93–96.
22. Shizukuda, Y. & Buttrick, P. M. (2002) *Am. J. Physiol.* **283**, L237–L238.
23. Hampton, M. B. & Winterbourn, C. C. (1995) *Free Radical Biol. Med.* **18,** 633–639.
24. Hennet, T., Richter, C. & Peterhans, E. (1993) *Biochem. J.* **289,** 587–592.
25. Sanchez-Alcazar, J. A., Ruiz-Cabello, J., Hernandez-Munoz, I., Pobre, P. S., de la Torre, P., Siles-Rivas, E., Garcia, I., Kaplan, O., Munoz-Yague, M. T. & Solis-Herruzo, J. A. (1997) *J. Biol. Chem.* **272,** 30167–30177.
26. Banki, K., Hutter, E., Gonchoroff, N. J. & Perl, A. (1999) *J. Immunol.* **162,** 1466–1479.
27. Jayanthi, S., Ordonez, S., McCoy, M. T. & Cadet, J. L. (1999) *Mol. Brain Res.* **72,** 158–165.
28. Moreno-Manzano, V., Ishikawa, Y., Lucio-Cazana, J. & Kitamura, M. (2000) *J. Biol. Chem.* **275,** 12684–12691.
29. Barros, L. F., Kanaseki, T., Sabirov, R., Morishima, S., Castro, J., Bittner, C. X., Maeno, E., Ando-Akatsuka, Y. & Okada, Y. (2003) *Cell Death Differ.* **10,** 687–697.
30. Hampton, M. B. & Orrenius, S. (1997) *FEBS Lett.* **414,** 552–556.
31. Ricci, J. E., Maulon, L., Luciano, F., Guerin, S., Livolsi, A., Mari, B., Breittmayer, J. P., Peyron, J. F. & Auberger, P. (1999) *Oncogene* **18,** 3963–3969.
32. Luciano, F., Ricci, J. E. & Auberger, P. (2001) *Oncogene* **20,** 4935–4941.
33. Bortner, C. D. & Cidlowski, J. A. (1999) *J. Biol. Chem.* **274,** 21953–21962.
34. Okada, Y. & Maeno, E. (2001) *Comp. Biochem. Physiol. A Physiol.* **130,** 377–383.
35. Vu, C. C. Q., Bortner, C. D. & Cidlowski, J. A. (2001) *J. Biol. Chem.* **276,** 37602–37611.